Multiple-Model Adaptive Estimation for Star Identification with Two Stars

Steven A. Szklany* and John L. Crassidis†

University at Buffalo, State University of New York, Amherst, NY, 14260-4400

In this paper a multiple-model adaptive estimation approach is presented for star identification using only measurement data from two stars within the spacecraft sensor field-of-view. Star identification algorithms typically require four or more stars in the field-of-view to make the data association with known cataloged values robustly. When the minimum number of stars condition is not met, these algorithms are unable to converge to a solution. Sensors with a narrow field-of-view or observing a sparsely populated target region both complicate the star identification process with the current algorithms. This paper demonstrates the feasibility of a multiple-model adaptive estimation approach for robust star identification based on image measurements from two stars in the field-of-view. The concept utilizes successive observations of the same two stars and their inter-star angle along with an understanding of the sensor noise statistics. The measurements are compared to a set of candidate cataloged star pairs to create a residual which updates likelihood estimates for each possible star pair. Simulation results show robust convergence of the likelihood estimates to the true star pair when the measurements are corrupted with Gaussian noise. The compact and computationally efficient implementation is well suited for onboard spacecraft operation.

I. Introduction

As the barrier to access space lowers, decreasing the complexity and cost of spacecraft navigation packages becomes more significant. Star trackers [1] have been historically made up a large percentage of the cost of a navigation sensor package. More economical star trackers or cameras possess a smaller field-of-view (FOV) which restricts the number of stars observable at any time. As noted in Ref. [2], often spacecraft are already equipped with science cameras which generally have a small FOV which could be used for star identification. Reference [2] presents an approach to address smaller FOVs by increasing the number of stars in the catalog to include dimmer stars, therefore increasing the observed stars in the FOV. This increases the size of the onboard catalog and the computational cost of the associated algorithms. Many of the star pattern recognition techniques mentioned in Ref. [3] require at least three stars for convergent identification with respect to an onboard star catalog. Therefore, if an inadequate number of stars is present in the FOV, the current algorithms can provide no identification solution. Limited fuel and energy resources on spacecraft often restrict the ability to reposition the spacecraft's FOV toward more populated star fields. By accepting less stringent star requirements, the probability of finding an attitude solution across different operating conditions increases.

Current methods to address observed star identification have evolved significantly over time. All methods attempt to match the observed star field with known characteristics of the star catalog. The size and complexity of star catalogs have also increased as more stars have been cataloged as well as more star attributes logged. Along with star inertial vectors, inter-star angles are recorded. The inter-star angle is the angle formed by the line-of-sight vectors between two stars. The "angle" method is leveraged in this work. The angle inference from two-star measurements can be shown to be attitude independent; therefore, there is

*Graduate Student, Department of Mechanical & Aerospace Engineering, University at Buffalo, State University of New York, Amherst, NY, 14260-4400. Email: sszklany@buffalo.edu. Member AIAA.

†CUBRC Professor in Space Situational Awareness, Department of Mechanical & Aerospace Engineering, University at Buffalo, State University of New York, Amherst, NY, 14260-4400. Email: johnc@buffalo.edu. Fellow AIAA.

no need for the spacecraft to be slewing during observation for the proposed method. The only requirement is that the stars stay within the FOV while the algorithm converges on the most likely star-pair solution.

Robust star identification algorithms do not require *a priori* knowledge of attitude and angular velocity, although Ref. [4] shows an approach to determine the angular velocity without identified stars. Without knowledge of spacecraft states, the star identification algorithm is qualified for lost-in-space conditions, where the spacecraft has no knowledge of its position or attitude. The proposed method leverages the known sensor statistics to estimate the most likely two-star solution. As successive observations are made, the number of likely star pairs reduces until the algorithm is shown to converge on a single, most likely star pair. Although the proposed method is most efficiently utilized when only two stars are present in the FOV, it still can be applied where more stars are visible. In that case, multiple star pair measurements can be used in multiple instances of the proposed algorithm.

Another critical aspect of star identification algorithms is computational efficiency. Given the growing size of star catalogs, searching catalog values becomes challenging with the limited onboard spacecraft computational resources. The presented method avoids matrix manipulations and costly catalog searches. Much of the traditional matrix manipulation of Kalman filtering has been simplified to scalar operations in the proposed two star identification method. The number of computations varies with the number of candidate stars selected. With regard to the catalog search, by utilizing the k-vector approach or Search-Less Algorithm developed in Ref. [5], the catalog angles are efficiently referenced in the proposed method. The catalog inter-star angles are sorted and accessed by a linear relationship which efficiently replaces search functions.

In this paper a Multiple-Model Adaptive Estimation (MMAE) approach [6] is incorporated to perform star identification with only two stars. MMAE uses a parallel bank of filters to provide multiple estimates, where each filter corresponds with a dependence on some unknowns, which can be the process or measurement noise covariance elements if desired. The state estimate, if desired, is provided through a sum of each filter's estimate weighted by the likelihood of the unknown elements conditioned on the measurement sequence. The likelihood function gives the associated hypothesis that each filter is the correct one. The MMAE approach is very robust for identification purposes because the likelihoods involve exponential functions. This quickly disregards observations whose likelihoods are small and amplifies those whose likelihoods are large, making it an ideal algorithm for star identification with only two stars.

The MMAE approach requires a time series of observations, and it is executed in real-time updating the likelihoods with each successive observation. This is one disadvantage over standard star pattern recognition methods, which use only one "snapshot" to identify stars. But these methods cannot perform an identification with only two stars in general. A topic which will be expanded on in future work is the data association problem of successive observations of the two stars in the FOV in the MMAE process. Data association refers to the operation ensuring that the two stars seen in the FOV are the same stars observed in previous observations. Tracking unknown and unmodeled objects stresses the estimation algorithm since there is no precise model to propagate states from measurement data. Another complication to data association is the handling of multiple targets. In the case of the two star identification process, the target tracking problem is reduced in scope. The Nearest Neighbor algorithm is the most straightforward approach to data association. The Nearest Neighbor algorithm described in Ref. [7] simply updates a track based on the closest observation. More sophisticated approaches will be investigated for this work such as the Global Nearest Neighbor and the Joint Probabilistic Data Association.

The organization of this paper is as follows. First a brief survey into star identification algorithms will be presented to highlight the applicability of the proposed star identification method. Second, the angle method for star identification will be explained as it pertains to the overall success of the presented star identification method. Then, the MMAE approach will be covered. Following that, the adaptation of the MMAE algorithm to two-star identification problem will be discussed. Simulation results are presented along with convergence trend analyses and chi-square test simulations. A performance comparison is also made against a traditional star identification technique to demonstrate performance against a known method. Finally, conclusions are drawn upon the developed theory and simulation results.

II. Star Identification Algorithms

High accuracy attitude pointing spacecraft missions rely heavily on the precision and robustness of star trackers and star identification algorithms. The function of star identification algorithms is to match the observed star FOV to that in a catalog which then provides the relationship between the body and inertial frames, or the attitude matrix.

Star identifications have evolved from methods which utilized *a priori* attitude information and pattern recognition of inter-star angles to generate autonomous attitude estimates [8]. By requiring some knowledge of attitude, the algorithm is unable to provide an attitude solution where no *a priori* knowledge existed. This condition is denoted the lost-in-space condition. This condition was not tractable until an algorithm was presented in Ref. [9]. The algorithm proposed in Ref. [9] uses the inter-star angle of three stars and the associated interior angle of the three stars for star recognition. The use of more information in the image provided extremely valuable in finding matching cataloged stars. Further work utilized more features within the image including triangle area (Ref. [10]) and improved search techniques (Ref. [5]). To the authors' knowledge, the proposed algorithm is intended to address a problem that has not been directly solved. As more features are being utilized in star catalogs and star identification algorithms, more stars are required to be in the FOV. This work is intended to address the problem where only two stars are present in the FOV.

A. Angle Method

The foundation of the angle method for star identification is the determination of the angle between two vectors pointing to stars in inertial space. The observed angle is then compared to a catalog populated with angles between associated star pairs. Matching the observed angle to the cataloged angle provides the link to positive identification. When considering the large number of stars in modern star catalogs, matching the exact angle is a computational challenge. The angle between vectors pointing to two stars is given by $\theta = \cos^{-1}(\mathbf{r}_1 \cdot \mathbf{r}_2)$ where $\mathbf{r}_1$ and $\mathbf{r}_2$ are unit star vectors given in inertial space. When utilizing star tracker images, the star vector observations are given in the body coordinate frame.

Star catalogs are populated with angles between neighboring pairs of stars. For the simulation cases presented here, only the star pairs with inter-star angles that fall within the sensor FOV are logged in the catalog. This reduction is to limit the catalog size to the physically realizable inter-star angle limit presented by the sensor.

B. Standard Deviation of Angle Measurement

Capturing sensor noise statistics is critical to the performance of many optimal filtering algorithms. In the case of star trackers, the sensor noise is applied to the observed position of the stars within the FOV yet residuals are taken based on observed inter-star angles. Clearly it is necessary to determine the relationship between point-wise sensor noise and resulting angle measurement variation. The variance of the angle measurement is a parameter critical to the success of the proposed two-star identification method. The method presented for developing the angle variance is followed from Ref. [10].

To begin, the standard coordinate transformation is expressed by $\mathbf{b}_i = A\mathbf{r}_i$ which illustrates the relationship between inertial star unit vector, $\mathbf{r}_i$ and the body star unit vector $\mathbf{b}_i$ related by the direction cosine matrix A. As described in Ref. [11], when measurement errors exist, the error is most probably concentrated in a small area in the direction of the direction of $A\mathbf{r}$. A sphere containing the error can be approximated by a tangent plane as shown by

$$\tilde{\mathbf{b}}_i = A\mathbf{r}_i + \mathbf{v}_i, \quad \mathbf{v}^T A\mathbf{r}_i = 0 \tag{1}$$

The sensor noise $\mathbf{v}_i$ is viewed as approximately Gaussian given by

$$E\{\mathbf{v}_i\} = \mathbf{0} \tag{2a}$$

$$R_i \equiv E\{\mathbf{v}_i\mathbf{v}_i^T\} = \sigma_i^2 \left[I_{3\times3} - (A\mathbf{r}_i)(A\mathbf{r}_i)^T \right] \tag{2b}$$

where $I_{3\times3}$ is a 3×3 identity matrix. Taking the dot product between stars $i = 1, 2$ yields the scaled representation of the angle between the two vectors. Substituting in $\tilde{\mathbf{b}}_i = A\mathbf{r}_i$ with no noise in Eq. (3) demonstrates the attitude-independency of the angle measurement:

$$\tilde{\mathbf{b}}_1^T\tilde{\mathbf{b}}_2 = \mathbf{r}_1^T A^T A\mathbf{r}_2 = \mathbf{r}_1^T\mathbf{r}_2 \tag{3}$$

The attitude independent angle measurement alleviates the need for nonzero angular body velocities as the measured angle will be the same regardless of the current attitude. Therefore, when collecting multiple observations of the same star pair, the sensor noise provides variation from frame to frame:

$$\tilde{\mathbf{b}}_i = A\mathbf{r}_i + \mathbf{v}_i, \quad i = 1,\, 2 \tag{4}$$

To determine the amount of variation in angle measurements that can be expected, the following derivation is developed. Beginning again with Eq. (4), the dot product is taken for stars $i = 1, 2$:

$$
\begin{aligned}
y &\equiv \tilde{\mathbf{b}}_1^T \tilde{\mathbf{b}}_2 \\
&= \mathbf{r}_1^T \mathbf{r}_2 + \mathbf{r}_1^T A \mathbf{v}_2 + \mathbf{r}_2^T A \mathbf{v}_1 + \mathbf{v}_1^T \mathbf{v}_2
\end{aligned}
\tag{5}
$$

Assuming that $\mathbf{v}_1$ and $\mathbf{v}_2$ are uncorrelated, the expectation of Eq. (5) is given by $E\{y\} = \mathbf{r}_1^T \mathbf{r}_2$. Define a new variable p:

$$
\begin{aligned}
p &\equiv y - E\{y\} \\
&= \mathbf{r}_1^T A^T \mathbf{v}_2 + \mathbf{r}_2^T A^T \mathbf{v}_1 + \mathbf{v}_1^T \mathbf{v}_2
\end{aligned}
\tag{6}
$$

Taking the expectation of p^2 will yield the variance of the angle measurement. Collecting the terms, the variance of the angle measurement given two noisy star body unit vector observations is given by

$$
\begin{aligned}
\sigma_p^2 &\equiv E\{p^2\} \\
&= \mathbf{r}_1^T A^T R_2 A \mathbf{r}_1 + \mathbf{r}_2^T A^T R_1 A \mathbf{r}_2 + \mathrm{Tr}(R_1 R_2) \\
&= \mathrm{Tr}(A \mathbf{r}_1 \mathbf{r}_1^T A^T R_2) + \mathrm{Tr}(A \mathbf{r}_2 \mathbf{r}_2^T A^T R_1) + \mathrm{Tr}(R_1 R_2)
\end{aligned}
\tag{7}
$$

where $E\{\mathbf{v}_1 \mathbf{v}_1^T\} = R_1$ and $E\{\mathbf{v}_2 \mathbf{v}_2^T\} = R_2$ which are represented in Eq. (2). Since there is no knowledge of the attitude A, the terms $A\mathbf{r}_1$ and $A\mathbf{r}_2$ are replaced by $\tilde{\mathbf{b}}_1$ and $\tilde{\mathbf{b}}_2$. As shown in Ref. [11], errors introduced by this substitution are second-order in nature.

As both the measurement and the variance of the inter-star angle has been shown to be attitude-independent, the two star identification algorithm can operate without any *a priori* knowledge of attitude or angular velocity. This is a critical distinction among star identification algorithms since it can provide attitude solutions where no current or previous attitude information is available (lost-in-space).

III. Multiple-Model Adaptive Estimation

The MMAE approach was first introduced in the mid-1960s [12]. Modern-day processors with parallel computing capabilities make an MMAE algorithm realistically possible today. The development of the MMAE process is followed from Ref. [6]. For the two star identification algorithm, further reductions in MMAE complexity provides a tractable solution for onboard spacecraft processing. The goal of the MMAE process is to determine the conditional probability density function (pdf) of the j^{th} element $\mathbf{p}^{(j)}$ given all the measurements. This pdf is not easily obtained, but Bayes' rule can be used to give a recursive formula:

$$
p(\mathbf{p}^{(j)} | \tilde{\mathbf{Y}}_k) = \frac{p(\tilde{\mathbf{Y}}_k | \mathbf{p}^{(j)})\, p(\mathbf{p}^{(j)})}{p(\tilde{\mathbf{Y}}_k)} = \frac{p(\tilde{\mathbf{Y}}_k | \mathbf{p}^{(j)})\, p(\mathbf{p}^{(j)})}{\displaystyle\sum_{j=1}^{M} p(\tilde{\mathbf{Y}}_k | \mathbf{p}^{(j)})\, p(\mathbf{p}^{(j)})}
\tag{8}
$$

where $\tilde{\mathbf{Y}}_k$ denotes the sequence of measurements $\{\tilde{\mathbf{y}}_0, \tilde{\mathbf{y}}_1, \ldots, \tilde{\mathbf{y}}_k\}$. It is desired to develop an update law that only is a function of the current measurement $\tilde{\mathbf{y}}_k$. To accomplish this task, the conditional probability equality and Bayes' rule are used to yield

$$
\begin{aligned}
p(\mathbf{p}^{(j)} | \tilde{\mathbf{Y}}_k) &= \frac{p(\tilde{\mathbf{y}}_k, \tilde{\mathbf{Y}}_{k-1}, \mathbf{p}^{(j)})}{p(\tilde{\mathbf{y}}_k, \tilde{\mathbf{Y}}_{k-1})} && \text{(9a)} \\
&= \frac{p(\tilde{\mathbf{y}}_k, \mathbf{p}^{(j)} | \tilde{\mathbf{Y}}_{k-1})\, p(\tilde{\mathbf{Y}}_{k-1})}{p(\tilde{\mathbf{y}}_k | \tilde{\mathbf{Y}}_{k-1})\, p(\tilde{\mathbf{Y}}_{k-1})} && \text{(9b)} \\
&= \frac{p(\tilde{\mathbf{y}}_k, \mathbf{p}^{(j)} | \tilde{\mathbf{Y}}_{k-1})}{p(\tilde{\mathbf{y}}_k | \tilde{\mathbf{Y}}_{k-1})} && \text{(9c)} \\
&= \frac{p(\tilde{\mathbf{y}}_k | \tilde{\mathbf{Y}}_{k-1}, \mathbf{p}^{(j)})\, p(\mathbf{p}^{(j)} | \tilde{\mathbf{Y}}_{k-1})}{\displaystyle\sum_{j=1}^{M} p(\tilde{\mathbf{y}}_k | \tilde{\mathbf{Y}}_{k-1}, \mathbf{p}^{(j)})\, p(\mathbf{p}^{(j)} | \tilde{\mathbf{Y}}_{k-1})} && \text{(9d)}
\end{aligned}
$$

For each $\mathbf{p}^{(j)}$ a set of state estimates is provided, denoted by $\hat{\mathbf{x}}_k^-(\mathbf{p}^{(j)}) \equiv \hat{\mathbf{x}}_k^{-(j)}$, usually through the bank of filters, such as a Kalman Filter (KF). Then, $p(\tilde{\mathbf{y}}_k|\tilde{\mathbf{Y}}_{k-1}, \mathbf{p}^{(j)})$ is given by $p\,(\tilde{\mathbf{y}}_k|\hat{\mathbf{x}}_k^{-(j)})$ because $\hat{\mathbf{x}}_k^{-(j)}$ uses all the measurements up to time point $k-1$, and it is a function of $\mathbf{p}^{(j)}$. Therefore, Eq. (9d) becomes

$$p\,(\mathbf{p}^{(j)}|\tilde{\mathbf{Y}}_k) = \frac{p\,(\tilde{\mathbf{y}}_k|\hat{\mathbf{x}}_k^{-(j)})\,p\,(\mathbf{p}^{(j)}|\tilde{\mathbf{Y}}_{k-1})}{\displaystyle\sum_{j=1}^{M} p\,(\tilde{\mathbf{y}}_k|\hat{\mathbf{x}}_k^{-(j)})\,p\,(\mathbf{p}^{(j)}|\tilde{\mathbf{Y}}_{k-1})} \tag{10}$$

Note that the denominator of Eq. (10) is just a normalizing factor to ensure that $p\,(\mathbf{p}^{(j)}|\tilde{\mathbf{Y}}_k)$ is a pdf. Defining $w_k^{(j)} \equiv p\,(\mathbf{p}^{(j)}|\tilde{\mathbf{Y}}_k)$ allows Eq. (10) to be rewritten as

$$\begin{aligned} w_k^{(j)} &= w_{k-1}^{(j)} p\,(\tilde{\mathbf{y}}_k|\hat{\mathbf{x}}_k^{-(j)}) \\ w_k^{(j)} &\leftarrow \frac{w_k^{(j)}}{\displaystyle\sum_{j=1}^{M} w_k^{(j)}} \end{aligned} \tag{11}$$

where $\leftarrow$ denotes replacement. Note that only the current time measurement $\tilde{\mathbf{y}}_k$ is needed to update the weights. The weights at time t_0 are initialized to $w_0^{(j)} = 1/M$ for $j = 1, 2, \ldots, M$. This is the traditional method for initializing weights in the MMAE. The next section discusses how the initial weight selection is improved to utilize information specific to the two star identification process. The convergence properties of the traditional MMAE are shown in Ref. [13], which assumes ergodicity in the proof.

The pdf $p\,(\tilde{\mathbf{y}}_k|\hat{\mathbf{x}}_k^{-(j)})$ is computed using the measurement residual $\mathbf{e}_k^{-(j)} \equiv \tilde{\mathbf{y}}_k - \hat{\mathbf{y}}_k^{-(j)}$, where $\hat{\mathbf{y}}_k^{-(j)} = H_k\hat{\mathbf{x}}_k^{-(j)}$. Note the MMAE is not restricted to linear systems, so that $\hat{\mathbf{y}}_k^{-(j)} = \mathbf{h}(\hat{\mathbf{x}}_k^{-(j)}, k)$ is applicable. The covariance of $\mathbf{e}_k^{-(j)}$ is given by

$$E_k^{-(j)} \equiv E\left\{\mathbf{e}_k^{-(j)}\mathbf{e}_k^{-(j)T}\right\} = H_k^{(j)} P_k^{-(j)} H_k^{(j)T} + R_k^{(j)} \tag{12}$$

where $P_k^{-(j)}$ is the covariance from the j^{th} filter. Then, $p\,(\tilde{\mathbf{y}}_k|\hat{\mathbf{x}}_k^{-(j)})$ is given by

$$p\,(\tilde{\mathbf{y}}_k|\hat{\mathbf{x}}_k^{-(j)}) = \frac{1}{\left[\det\left(2\pi E_k^{-(j)}\right)\right]^{1/2}} \exp\left\{-\frac{1}{2}\mathbf{e}_k^{-(j)T}\left(E_k^{-(j)}\right)^{-1}\mathbf{e}_k^{-(j)}\right\} \tag{13}$$

which is used in Eq. (11).

For the traditional MMAE, the conditional mean estimate is the weighted sum of the parallel filter estimates:

$$\hat{\mathbf{x}}_k^+ = \sum_{j=1}^{M} w_k^{(j)}\hat{\mathbf{x}}_k^{+(j)} \tag{14}$$

Also, the covariance of the state estimate can be computed using

$$P_k^+ = \sum_{j=1}^{M} w_k^{(j)}\left[\left(\hat{\mathbf{x}}_k^{+(j)} - \hat{\mathbf{x}}_k^+\right)\left(\hat{\mathbf{x}}_k^{+(j)} - \hat{\mathbf{x}}_k^+\right)^T + P_k^{+(j)}\right] \tag{15}$$

The state and covariance estimates suggest an output which is a combination of the M models. For the two star identification process, the goal is to converge on a single, discrete star pair, therefore the individual model outputs will not be combined as shown here. The specific estimate for $\mathbf{p}$ at time t_k, denoted by $\hat{\mathbf{p}}_k$, and error covariance, denoted by $\mathcal{P}_k$, are given by

$$\hat{\mathbf{p}}_k = \sum_{j=1}^{M} w_k^{(j)}\mathbf{p}^{(j)} \tag{16a}$$

$$\mathcal{P}_k = \sum_{j=1}^{M} w_k^{(j)}\left(\mathbf{p}^{(j)} - \hat{\mathbf{p}}_k\right)\left(\mathbf{p}^{(j)} - \hat{\mathbf{p}}_k\right)^T \tag{16b}$$

Equation (16b) can be used to define 3σ boundaries on the estimate $\hat{\mathbf{p}}_k$. If M is large and the significant regions of the parameter space of $\mathbf{p}$ are well represented by $\mathbf{p}^{(j)}$, then Eq. (16a) is obviously a good approximation of the conditional mean of $\mathbf{p}$.

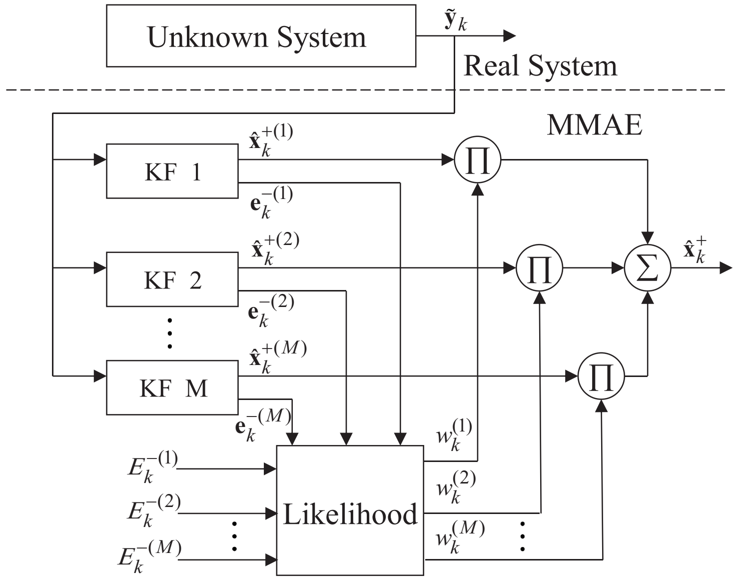

Figure 1. Multiple-Model Adaptive Estimation Process

An overview of the MMAE process is shown in Figure 1. Each filter has a different assumed model which is parameterized using $\mathbf{p}^{(j)}$; these parameters may be model parameters or other parameters, such as elements of the process noise covariance or measurement noise covariance. All filters are executed in parallel. The covariance of each filter is used to develop the covariance of the individual residual, given by Eq. (12). The posterior pdf in Eq. (13) is computed, and the weight for each filter is computed using Eq. (11). The MMAE state estimate and its covariance are computed using Eq. (14) and (15), respectively, and the MMAE parameter estimate and its covariance are computed using Eq. (16a) and (16b), respectively.

Additional methods of enhancing the traditional MMAE process include Interacting MMAE [6]. Interacting MMAE fuses discrete model outputs to generate a most-likely state and covariance estimate. For this stage of the work, it is assumed that the stars in the FOV are found within the star catalog, therefore keeping discrete and unique star pair possibilities invalidates any need for an Interacting MMAE approach. The most likely solution is not a combination or fusion of the star pair angles in a catalog, but a single, discrete star pair.

IV. MMAE for Two Star Identification

The proposed algorithm provides a method to converge on the most likely star-pair solution given only information about the sensor noise and multiple observations of the same stars. The algorithm is modular to fit a wide range of candidate star pairs that are pulled from the catalog. Candidate star pairs are selected based on the measured angle and the assumed sensor noise. As compared to the traditional MMAE, the MMAE for two-star identification modifies the data flow slightly. Figure 2 shows the filter models have been replaced by candidate star pairs and the residual is the only output from each model.

The input to each model is the measured inter-star angle. Upon receiving the first two-star observation, the inter-star dot product is calculated by

$$\tilde{y}_k = \tilde{\mathbf{b}}_{1_k}^T \tilde{\mathbf{b}}_{2_k} \tag{17}$$

where $\tilde{\mathbf{b}}_{1_k}$ and $\tilde{\mathbf{b}}_{2_k}$ are the unit vectors of the two observed stars at time t_k. The dot product produces a scalar value for each model $j = 1, 2, \ldots, M$. Instead of the filter outputting a covariance matrix at each time step, the variance is captured by the angle measurement variance. The variance, σ_k^2 is calculated at

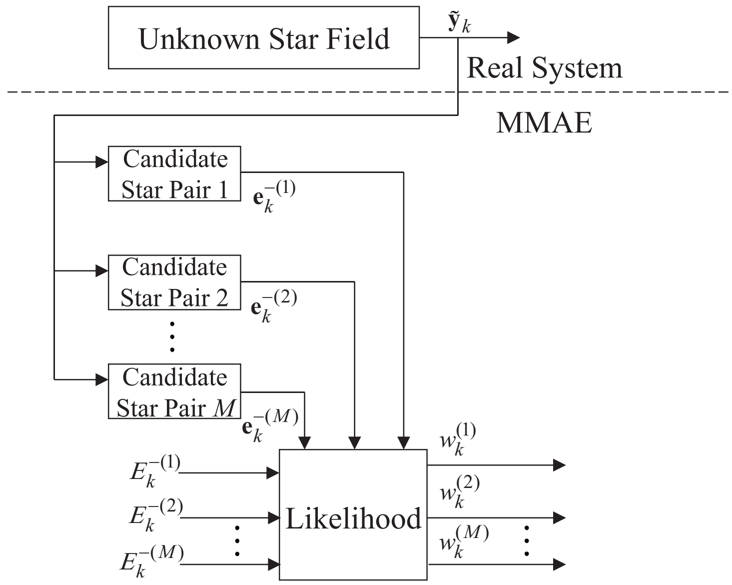

Figure 2. Multiple-Model Adaptive Estimation for Two-Star Identification

time t_k which is repeated from Eq. (7):

$$\sigma_k^2 = \mathrm{Tr}(\tilde{\mathbf{b}}_{1_k}\tilde{\mathbf{b}}_{1_k}^T R_{2_k}) + \mathrm{Tr}(\tilde{\mathbf{b}}_{2_k}\tilde{\mathbf{b}}_{2_k}^T R_{1_k}) + \mathrm{Tr}(R_{1_k} R_{2_k}) \tag{18}$$

The candidate star pairs need to be populated intelligently to limit the number of possible outcomes to only those which lie within the statistical limits of the observation. To determine the candidate star pairs in the catalog, the variance is used to create a symmetrical boundary around the observed dot product. The number of standard deviations to search around the observed dot product can be determined by the user, but if $\pm 3\sigma$ is chosen, then the true value will be contained within that range 99.7% of the time. The penalty for a high probability of capturing the true value is the large number of candidate star pairs. Although the MMAE algorithm efficiently handles any number of candidate star pairs, there is additional calculations due to the wide search range.

With the candidate star pairs identified, the MMAE process is initialized with weighting factors for each star pair. Traditionally, MMAE algorithms use an equal initial weight for all M models. In the case of the two-star identification MMAE, the star pairs are pulled from a catalog with a distribution, therefore the algorithm can reflect that statistical distribution on its initial weight factor. The weight for each candidate star pair will be a function of its difference from the measured angle and the variance. The initial weights are generated by the following:

$$f\left(\mathbf{r}_1^{(j)T}\mathbf{r}_2^{(j)}\right) = \frac{1}{\sqrt{2\pi\sigma^2}}\exp\left\{-\frac{(\tilde{\mathbf{b}}_1^T\tilde{\mathbf{b}}_2 - \mathbf{r}_1^{(j)T}\mathbf{r}_2^{(j)})^2}{2\sigma^2}\right\} \tag{19a}$$

$$w_1^{(j)} = \frac{f\left(\mathbf{r}_1^{(j)T}\mathbf{r}_2^{(j)}\right)}{\sum_{j=1}^{M} f\left(\mathbf{r}_1^{(j)T}\mathbf{r}_2^{(j)}\right)} \tag{19b}$$

Equations (19) depicts the Gaussian distribution as it applies to the initial weights. Since each individual model of the MMAE represents possible star pairs, the residual from the candidate star pair is the difference between the observed body angle and the static catalog angle for star pairs $j = 1, 2, \ldots, M$. Here, M is the number of candidate star pairs for a given two-star observation. The residual calculation for each candidate star pair, j, is represented by

$$e_k^{(j)} = \tilde{\mathbf{b}}_{1_k}^T\tilde{\mathbf{b}}_{2_k} - \mathbf{r}_1^{(j)T}\mathbf{r}_2^{(j)} \tag{20}$$

At each time step t_k, a new residual is calculated for each candidate pair given the measurements $\tilde{\mathbf{b}}_{1_k}$ and $\tilde{\mathbf{b}}_{2_k}$. The measurement variance is updated at each time step with the current measurement and assumed sensor noise standard deviation. The variance is equal for all possible candidate star pairs. Equation (18) describes the calculation for measurement angle variance.

With the residual and the measurement variance defined, the likelihood and weighting functions of the MMAE process can be developed. The likelihood function assumes a Gaussian distribution of the noise of the angle measurement. Equation (21) describes the relationship between the angle residual and the likelihood for each j candidate star pair. The residual and variance are scalar values for each candidate star pair $j = 1, 2, \ldots, M$ therefore there is a simplification in notation compared to traditional MMAE equations:

$$p(\tilde{\mathbf{y}}_k|\mathbf{x}_k^{(j)}) = \frac{1}{(2\pi\sigma_k^2)^{1/2}} \exp\left\{-\frac{\left(e_k^{(j)}\right)^2}{2\sigma_k^2}\right\} \tag{21}$$

For each time, k, the residual $e_k^{(j)}$ and the likelihood $p(\tilde{\mathbf{y}}_k|\hat{\mathbf{x}}_k^{-(j)})$ are updated with new inter-star angle measurements. The weight is updated at each time k for candidate star pairs $j = 1, 2, \ldots, M$ with those values according to

$$\begin{aligned} w_k^{(j)} &= w_{k-1}^{(j)} p\left(\tilde{\mathbf{y}}_k|\mathbf{x}_k^{(j)}\right) \\ w_k^{(j)} &\leftarrow \frac{w_k^{(j)}}{\sum\limits_{j=1}^{M} w_k^{(j)}} \end{aligned} \tag{22}$$

Table 1 summarizes the MMAE algorithm for two-star identification.

V. Simulation Results

The MMAE two-star identification algorithm is capable of identifying correct star pairs from a very dense candidate star pair angle sample. As the size of the star catalog increases, the difference between inter-star angles decreases as more samples populate the catalog. The dense candidate star angle list challenges the robustness and accuracy of the MMAE two-star identification algorithm. The simulation parameters are defined in Table 2. Figure 3 illustrates the difference between candidate star angles selected from the $\pm 3\sigma$ range around an observed inter-star angle. To illustrate the densely populated candidate star pairs, the selected limits yield 110 possible star pairs with many of the candidate star pair angles differing less than 5μrad from adjacent inter-star angles. For all simulation cases presented, the spacecraft is assumed to be stationary while observing the star field.

The initial measurement for inter-star angle is used to generate the $\pm 3\sigma$ bounds and extracting the valid candidate star pairs from the catalog data. In the case presented here, there are 91 valid candidate star pairs selected after the first measurement of inter-star angle. The k-vector approach from Ref. [5] is used to select the candidate star pairs from the catalog. Figure 4 illustrates the k-vector approach with inter-star dot products from the catalog. The search process is reduced drastically by the k-vector method as it works on a sorted catalog and determines the desired catalog values based on the linear parameters set for the catalog. With the candidate selected, the algorithm can begin updating weights with new measurements after each observation.

Figure 5 illustrates the weight convergence on the correct star pair given 91 possible star pair combinations. The algorithm converges on the solution within 60 seconds of the first observation. The weighting factors are utilized as the indication of convergence as a weight value of 1 signals the most likely solution. Considering no other algorithm could provide an attitude solution in this condition, the convergence time is very acceptable.

VI. Convergence Observations

Further simulations which use randomly pointed line-of-sight vectors in the star field uncover a range of star pair convergence times. To determine the sensitivity, further convergence analyses are investigated.

Table 1. MMAE for Two Star Identification Algorithm

Initial Observation	$y_k = \tilde{\mathbf{b}}_{1_k}^T \tilde{\mathbf{b}}_{2_k}$
Variance	$\sigma_k^2 = \mathrm{Tr}(\tilde{\mathbf{b}}_{1_k} \tilde{\mathbf{b}}_{1_k}^T R_{2_k}) + \mathrm{Tr}(\tilde{\mathbf{b}}_{2_k} \tilde{\mathbf{b}}_{2_k}^T R_{1_k}) + \mathrm{Tr}(R_{1_k} R_{2_k})$
Reduce Field	$y_{\max} = \tilde{\mathbf{b}}_{1_k}^T \tilde{\mathbf{b}}_{2_k} + 3\sigma_k$ $y_{\min} = \tilde{\mathbf{b}}_{1_k}^T \tilde{\mathbf{b}}_{2_k} - 3\sigma_k$
Initialize Weights	$f\left(\mathbf{r}_1^{(j)T} \mathbf{r}_2^{(j)}\right) = \frac{1}{\sqrt{2\pi\sigma^2}} \exp\left\{-\frac{(\tilde{\mathbf{b}}_1^T \tilde{\mathbf{b}}_2 - \mathbf{r}_1^{(j)T} \mathbf{r}_2^{(j)})^2}{2\sigma^2}\right\}$ $w_1^{(j)} = \frac{f\left(\mathbf{r}_1^{(j)T} \mathbf{r}_2^{(j)}\right)}{\sum_{j=1}^{M} f\left(\mathbf{r}_1^{(j)T} \mathbf{r}_2^{(j)}\right)}$
Residual	$e_k^{(j)} = \tilde{\mathbf{b}}_{1_k}^T \tilde{\mathbf{b}}_{2_k} - \mathbf{r}_1^{(j)T} \mathbf{r}_2^{(j)}$
Likelihood	$p(\tilde{\mathbf{y}}_k \mid \mathbf{x}_k^{(j)}) = \frac{1}{(2\pi\sigma_k^2)^{1/2}} \exp\left\{-\frac{\left(e_k^{(j)}\right)^2}{2\sigma_k^2}\right\}$
Update Weights	$w_k^{(j)} = w_{k-1}^{(j)} p\left(\tilde{\mathbf{y}}_k \mid \mathbf{x}_k^{(j)}\right)$ $w_k^{(j)} \leftarrow \frac{w_k^{(j)}}{\sum_{j=1}^{M} w_k^{(j)}}$

Table 2. Simulation Parameters

Sample Rate	10 Hz
Field of View	6°
Noise StdDev	2.9e−5
Star Catalog Size	4000 Stars
Angle Catalog Size	40726 Angles

Two similar simulations are performed that yield different convergence times. The first simulation has 84 candidate star pairs for the observed inter-star angle. The second is another simulation with 85 candidate star pairs. Figures 6(a) and 6(b) show the weights over time as the short convergence case converges on the correct pair in about 60 seconds while the long convergence case picks the correct star pair in 300 seconds. The cause of the different convergence rates is the distribution of the candidate inter-star angles and the observed inter-star angle.

For illustration purposes, the measured angle is averaged over time. This produces a slowly converging waveform that is dependent on the noise of the sensor. As more samples are taken, the variance of average narrows. This directly reflects the concept of the Chebyshev Inequality. As shown in Ref. [14] with $k > 0$,

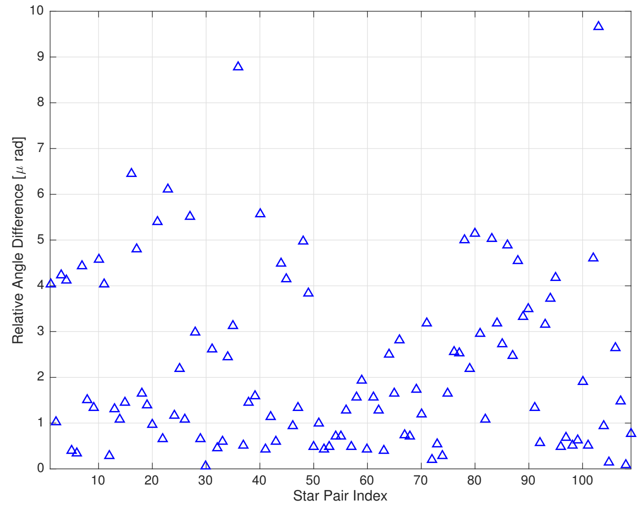

Figure 3. Relative Angle Difference Between Candidate Star Pairs

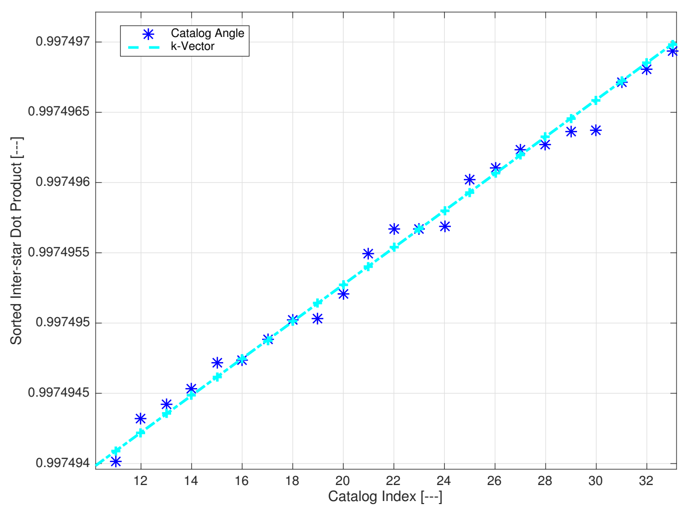

Figure 4. k-Vector Inter-Star Angle Selection

the probability of the random variable $\mathbf{x}$ being greater than a distance $k\sigma$ greater than the expectation, $E(\mathbf{x})$, is less than or equal to $1/k^2$:

$$p(\|\mathbf{x} - E(\mathbf{x})\| \geq k\sigma) \leq \frac{1}{k^2} \tag{23}$$

As more samples, k, are taken, the running average converges on the expected value. With more densely populated candidate star arrays, the average needs to converge to very small values to be able to discern a most likely solution, therefore taking longer for overall convergence.

Another way to visualize the convergence condition is to take the average of the measured inter-star angle at each time step. As that average converges on the expected value or mean, it encounters potential candidate inter-star angles. Figures 7(a) and 7(b) illustrate the experiment to validate convergence times in the two star identification algorithm. The averaged measured value is shown in blue while the red horizontal traces represent individual candidate star dot products. The plot is zoomed to show the relevant data, therefore not all candidate star dot products are visible. The short converging cases show the average of

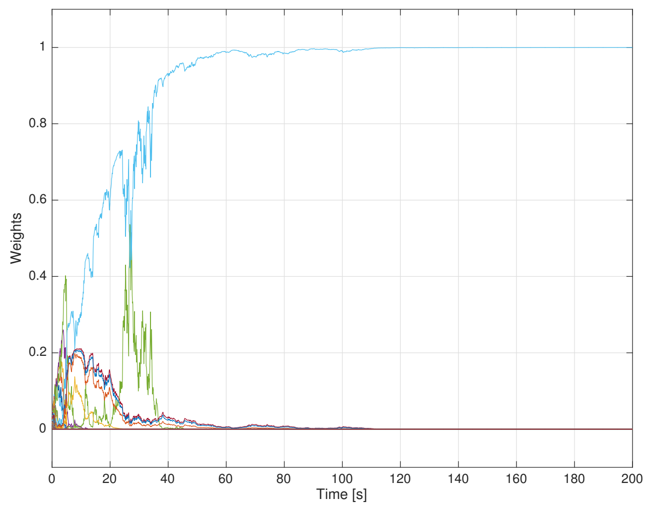

Figure 5. MMAE Weight Convergence for 91 Candidate Star Pairs

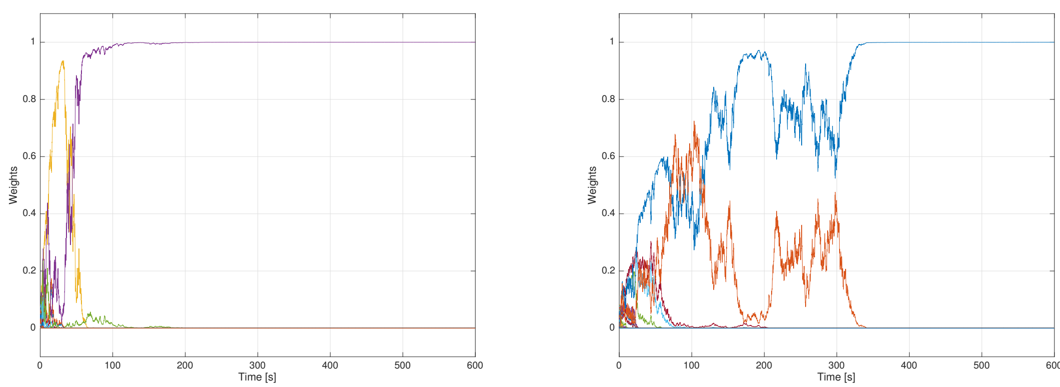

(a) **Short Convergence**

(b) **Long Convergence**

Figure 6. Convergence Comparison

the dot product to zero on a candidate star angle quickly. Surrounding candidate star pairs in the short converging case are spread away from the true value. For the long converging case, the average hovers in between two possible star pairs before finally converging on the true value later in the time series. The distribution of the candidate star pairs around the true value dictates how many samples are required to further refine the running average of the inter-star angle.

As illustrated, the convergence of the two star identification algorithm is dependent on the density of the candidate inter-star angles and the noise statistics of the sensor. Changing the star tracker sample rate will also influence the convergence time. Slower sample rates will increase convergence times as it takes longer to average the noise of the observed angle. Given the difficult conditions for convergence, the proposed approach has been shown to provide a very robust and efficient method for identifying two stars.

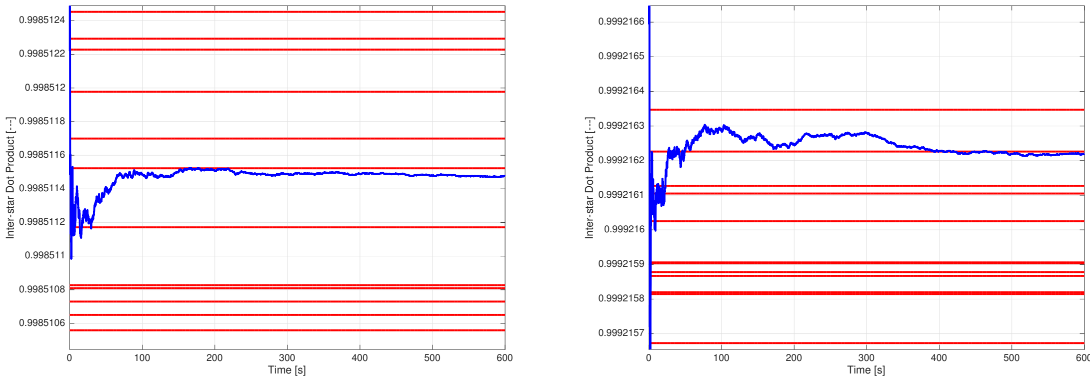

(a) **Average Dot Product and Candidate Star Pairs, Short Convergence**

(b) **Average Dot Product and Candidate Star Pairs, Long Convergence**

Figure 7. Average Dot Product Convergence and Candidate Star Pair Density

A. Chi-Square Test

The chi-square distribution is often used to provide a consistency test in estimators, which is useful to determine whether or not reasonable state estimates are provided. In the case of the MMAE two star identification, the residuals for each candidate star pair can be evaluated via the chi-square test. Assuming a Gaussian distribution for the $n \times 1$ vector $\mathbf{x}$, with mean $\boldsymbol{\mu}$ and covariance R, the following variable is said to have a chi-square distribution with n degrees of freedom (DOF):

$$q = (\mathbf{x} - \boldsymbol{\mu})^T R^{-1} (\mathbf{x} - \boldsymbol{\mu}) \tag{24}$$

The variable q is the sum of squares of n independent zero-mean variables with variance equal to one. This can be shown by defining the following variable [15]:

$$\mathbf{u} \equiv R^{-1/2} (\mathbf{x} - \boldsymbol{\mu}) \tag{25}$$

Then, $\mathbf{u}$ is clearly Gaussian with $E\{\mathbf{u}\} = \mathbf{0}$ and $E\left\{\mathbf{u}\,\mathbf{u}^T\right\} = I$. The chi-square distribution is written as

$$q \sim \chi_n^2 \tag{26}$$

The mean and variance are given by

$$E\{q\} = \sum_{i=1}^{n} E\left\{u_i^2\right\} = n \tag{27a}$$

$$E\left\{(q-n)^2\right\} = \sum_{i=1}^{n} E\left\{(u_i^2 - 1)^2\right\} = \sum_{i=1}^{n} (3 - 2 + 1) = 2n \tag{27b}$$

where the relationship $E\left\{x^4\right\} = 3\sigma^4$ has been used for the term involving u_i^4.

The chi-square density function with n DOF is given by

$$p(q) = \frac{1}{2^{n/2}\Gamma(n/2)}\, q^{\frac{n-2}{2}} e^{-\frac{q}{2}} \tag{28}$$

where the gamma function Γ is defined as

$$\Gamma\left(\frac{1}{2}\right) = \sqrt{\pi} \tag{29a}$$

$$\Gamma(1) = 1 \tag{29b}$$

$$\Gamma(m+1) = m\,\Gamma(m) \tag{29c}$$

Tables of points on the chi-square distribution can be found in Ref. [16]. For DOF's above 100, the following approximation can be used:

$$\chi_n^2(1-Q) = \frac{1}{2}\left[\mathcal{G}(1-Q) + \sqrt{2n-1}\right]^2 \tag{30}$$

where $\chi_n^2(1-Q)$ indicates that to the left of a specific point, the probability mass is $1-Q$. An important quantity used in consistency tests is the 95% *two-sided probability region* for an $N(0,1)$ random variable:

$$[\mathcal{G}(0.025),\, \mathcal{G}(0.975)] = [-1.96,\, 1.96] \tag{31}$$

Other values for $\mathcal{G}$ can be found in Ref. [15]. Then, specific values can be calculated for $\chi_n^2(1-Q)$ using Eq. (30).

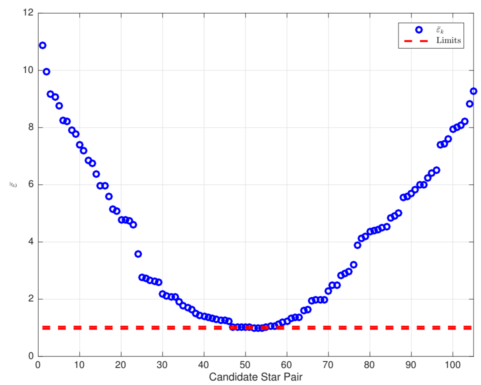

(a) **Plot of $\bar{\varepsilon}_k^{(j)}$ for 105 Candidate Stars**

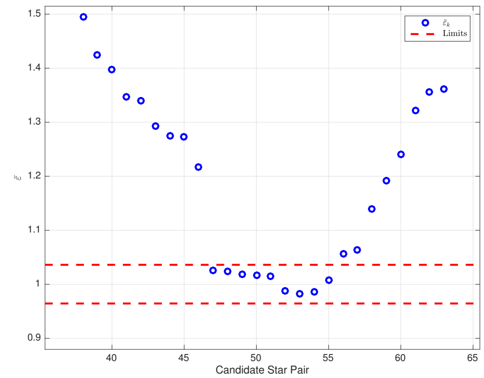

(b) **Rescaled Plot of $\bar{\varepsilon}_k^{(j)}$**

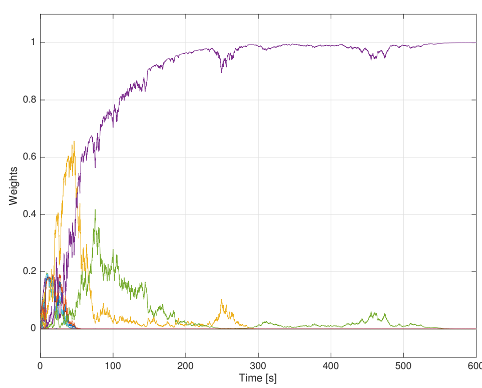

(c) **Convergence of Weights for Chi-Square Test Simulation**

Figure 8. Convergence of Weights for Chi-square Test Simulation

For M Monte Carlo runs, the average normalized error square is computed for each candidate star pair. Derived from Eq. (24) the average normalized error square is represented by

$$\bar{\varepsilon}_k^{(j)} = \frac{1}{M}\sum_{i=1}^{M} \varepsilon_k^{(j)}(i) = \frac{1}{M}\sum_{i=1}^{M} \frac{(\mathbf{e}_k^{-(j)}(i))^2}{E_k^{-(j)}(i)} \tag{32}$$

The term $\mathbf{e}_k^{-(j)}$ represents the angle residual as calculated in Eq. (20). The hypothesis is accepted if the following is true:

$$\bar{\varepsilon}_k \in [\zeta_1, \zeta_2] \tag{33}$$

Constants ζ_1 and ζ_2 are derived from the tail probabilities of the chi-square density. For the simulation results, $M = 6000$ and using Eq. (30), $\zeta_1 = 0.9645$ and $\zeta_2 = 1.0360$. Figures 8(a), 8(b), and 8(c) illustrates the resulting chi-square test given a sample simulation with 105 candidate star pairs.

As Figure 8(b) shows, there are multiple candidate star pair combinations that satisfy the chi-square test conditions, but the weight plot shows the convergence on the correct star pair. This again demonstrates the challenge of identifying a single star pair from angle-only measurements. The density of the candidate star pairs provide a difficult estimation problem as the estimated value needs to decipher between very small differences. The fact that the weights are able to converge on the correct star pair demonstrates the robustness of the two star identification algorithm. The MMAE process benefits from the exponential function in the likelihood equation which increases the algorithms sensitivity to differences in the residuals.

VII. Comparison to Traditional Star Identification

To evaluate the applicability of the MMAE two-star algorithm, a traditional star identification algorithm is run in parallel to determine its performance with the same noisy, two-star measurement data. Since only two stars are available in the FOV, the angle method is the only applicable algorithm benchmark. Typically, the angle method requires a nonzero number of pivots to provide the correct solution. The ambiguity of a single angle measurement requires additional FOV measurements to reduce the candidate star pairs therefore, pivoting requires greater than two stars in the FOV. In this case, the success will be limited to cases where it can provide a likely solution based given a rather unique measured angle, i.e. one that does not have similar candidate pairs within the variance of the measurement. If multiple solutions exist due to measurement uncertainty, the angle method will be unable to pivot to reduce the candidate pairs, therefore it would output an inconclusive identification.

At each time step, the measured stars in the FOV are fed to both the MMAE star identification algorithm as well as the angle method. For the angle method, each measurement is treated as a new observation. Since no pivoting is possible, the number of candidate star pairs resulting from the angle method is collected. Figure 9 illustrates the convergence of the MMAE star identification algorithm as well as the inability of the angle method to provide a single conclusive star pair. The MMAE is able to innovate the current candidate weights and converge on the correct star pair while the angle method contains a list varying around 100 possible star pairs. Without additional stars in the FOV, the angle method cannot trim the list of candidate star pairs. The angle method comparison further strengthens the applicability and usefulness of the MMAE star identification algorithm in conditions where only two stars are available in the FOV.

VIII. Conclusions and Future Work

A new approach to identify only two observed stars in the field-of-view was presented in this paper. The angle method for star identification was explained and the associated statistical error analysis was described. The Multiple-Model Adaptive Estimation (MMAE) approach was also developed. The modifications made to the MMAE process to perform star identification tasks were presented along with simulation results. The MMAE for two star identification was shown to robustly converge on the correct star pair given a large number of densely populated candidate star pairs. Further analysis was performed to determine the algorithms sensitivity to convergence. It was shown that the density around the true angle of the candidate star pair angles contribute to the overall algorithm convergence. Future work is planned to ensure the data association of successive star observations is addressed. False stars and non-cataloged star tests need to be performed to ensure robustness, as well as robustness tests to noise statistics of the star camera. In addition, this technique can be applied to FOVs containing greater than two stars. Multiple instances of the MMAE Star ID algorithm can be run for each observed star pair in parallel. If a star is lost or leaves the field of view during observation, the remaining stars in the FOV can be used for convergence.

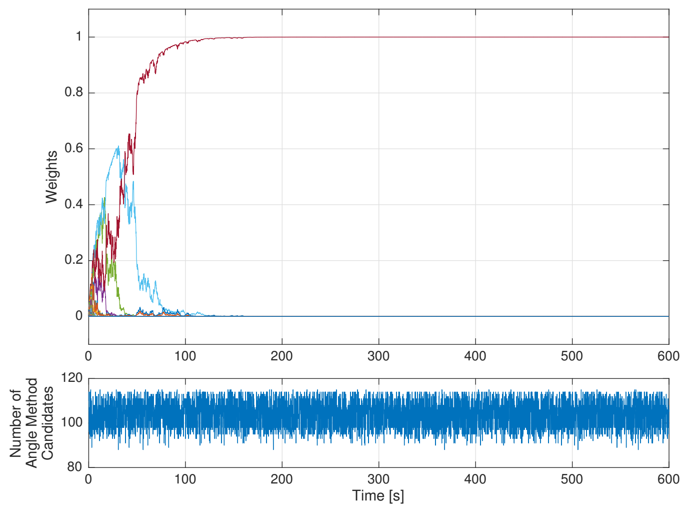

Figure 9. Comparison of MMAE Convergence and Individual Outputs of Angle Method

References

[1]Markley, F. L. and Crassidis, J. L., *Fundamentals of Spacecraft Attitude Determination and Control*, Springer, New York, NY, 2014, pp. 125–133, doi:10.1007/978-1-4939-0802-8.

[2]Clouse, D. S. and Padgett, C. W., "Small Field-of-View star Identification Using Bayesian Decision Theory," *IEEE Transactions on Aerospace and Electronic Systems*, Vol. 36, No. 3, July 2000, pp. 773–783, doi:10.1109/7.869495.

[3]Spratling, B. B. and Mortari, D., "A Survey on Star Identification Algorithms," *Algorithms*, Vol. 2, No. 1, Jan. 2009, pp. 93–107, doi:10.3390/a2010093.

[4]Crassidis, J. L., "Angular Velocity Determination Directly from Star Tracker Measurements," *Journal of Guidance, Control, and Dynamics*, Vol. 25, No. 6, Nov.-Dec. 2002, pp. 1165–1168, doi:10.2514/2.4999.

[5]Mortari, D., "Search-Less Algorithm for Star Pattern Recognition," *The Journal of the Astronautical Sciences*, Vol. 45, No. 2, 1997, pp. 179–194.

[6]Crassidis, J. L. and Junkins, J. L., *Optimal Estimation of Dynamic Systems*, CRC Press, Boca Raton, FL, 2nd ed., 2012, pp. 249–256.

[7]Blackman, S. S., "Multiple Hypothesis Tracking for Multiple Target Tracking," *IEEE Aerospace and Electronic Systems Magazine*, Vol. 19, No. 1, Jan. 2004, pp. 5–18, doi:10.1109/MAES.2004.1263228.

[8]Junkins, J. L., White, C. C., and Turner, J. D., "Star Pattern Recognition for Real Time Attitude Determination," *The Journal of the Astronautical Sciences*, Vol. 25, No. 3, 1977, pp. 251–270.

[9]Liebe, C. C., "Pattern Recognition of Star Constellations for Spacecraft Applications," *IEEE Aerospace and Electronic Systems Magazine*, Vol. 8, No. 1, Jan. 1993, pp. 31–39, doi:10.1109/62.180383.

[10]Cole, C. L. and Crassidis, J. L., "Fast Star-Pattern Recognition Using Planar Triangles," *Journal of Guidance, Control, and Dynamics*, Vol. 29, No. 1, Jan.-Feb. 2006, pp. 64–71, doi:10.2514/1.13314.

[11]Shuster, M. D., "Maximum Likelihood Estimation of Spacecraft Attitude," *The Journal of the Astronautical Sciences*, Vol. 37, 1989, pp. 79–88.

[12]Magill, D. T., "Optimal Adaptive Estimation of Sampled Stochastic Processes," *IEEE Transactions on Automatic Control*, Vol. 10, No. 4, Oct. 1965, pp. 434–439, doi:10.1109/TAC.1965.1098191.

[13]Anderson, B. D. O. and Moore, J. B., *Optimal Filtering*, Prentice Hall, Englewood Cliffs, NJ, 1979, pp. 270–273.

[14]Maybeck, P. S., *Stochastic Models, Estimation, and Control*, Vol. 1, Academic Press, New York, NY, 1979, p. 151.

[15]Bar-Shalom, Y., Li, X. R., and Kirubarajan, T., *Estimation with Applications to Tracking and Navigation*, John Wiley & Sons, New York, NY, 2004, p. 58.

[16]Freund, J. E. and Walpole, R. E., *Mathematical Statistics*, Prentice Hall, Englewood Cliffs, NJ, 4th ed., 1987, p. 576.